

Exposure to Bisphenol A Upgrades Apoptosis, Inflammation and Fibrosis in Adult Rat Heart with Possible Amelioration Following Recovery

Original
Article

Amal S. Sewelam, Eman M. A. Abdelghany and Mohamed Ahmed Sabry

Department of Human Anatomy & Embryology, Faculty of Medicine, Zagazig University, Egypt

ABSTRACT

Introduction: Bisphenol A (BPA) is an environmental contaminant with a global use as a plasticizer. Daily BPA exposure begins early prenatally and continues throughout a person's life without exact limit or safety raising alarms concerning overall health.

Objective: To explore potential cardiotoxicity of orally administered BPA in adult rat, and to assess the outcome of recovery period following BPA stoppage.

Materials and Methods: Forty-eight adult male albino rats were allocated into four groups (12 each); control negative, control positive, BPA-treated and recovered. For eight weeks, rats in the 3rd group received daily BPA (50 mg/kg body weight, via oral gavage). In the recovery group, animals obtained BPA, for the same dose and duration similar to that in the 3rd group, then left to convalesce without BPA administration for 4 weeks. At the experimental end, blood was collected to estimate serum Creatine kinase-MB(CK-MB) level and heart specimens were handled for histology, immunohistochemistry, and quantitative morphometry study.

Results: BPA persuaded several histological, immunohistochemical and biochemical alterations manifested as cardiac fiber disruption, vascular congestion, hemorrhage, RBCs extravasation, inflammatory cell infiltration and fibrosis. Cardiomyocytes displayed dark acidophilic sarcoplasm, pyknosis and perinuclear vacuolation. Also, the mean area % for collagen fiber deposition, glycogen content, Bcl-2-associated X protein, Nuclear factor kappa B (NF- κ B) and Vimentin immune-expressions were significantly high. Furthermore, mast cell number/mm², MDA and CK-MB levels were enhanced meanwhile SOD, GSH and CAT levels were declined. After 4-week recovery, cardiomyocytes and vascular changes exhibited marked improvement and all previous metrics were directed toward normal values, though most of them were still demonstrating low significant differences contrasted to controls.

Conclusion: BPA induced cardiac structural and functional alterations via ROS generation, apoptosis, inflammation and fibrosis with considerable self-recovery following BPA cessation denoting transitory adverse impact. However, the particular mechanisms underlying cardiotoxicity or recovery still require further study.

Received: 14 January 2023, **Accepted:** 09 March 2023

Key Words: Bax, bisphenol A, heart, NF- κ B, vimentin.

Corresponding Author: Amal S. Sewelam, MD, Department of Human Anatomy & Embryology, Faculty of Medicine, Zagazig University, Egypt, **Tel.:** +20 11 5578 9552, **E-mail:** amalsolimansewelam@gmail.com

ISSN: 1110-0559, Vol. 47, No. 1

INTRODUCTION

Millions of tons of plastics are produced annually all over the world. Humans are continuously exposed to these hazardous environmental contaminants on a daily basis and life-long without even realizing them. Bisphenol A is an organic plasticizer principally applied to synthesize polycarbonate plastics and epoxy resin monomers. Polycarbonate plastics are commonly used in many customer products such as baby and water bottles, toys, plastic food containers, sports equipment, compact discs (CDs, DVDs), medical devices and dental sealants. Also, BPA based epoxy resin polymers are utilized as a protecting inner coating for metallic canned food and beverage containers as well as for water supply pipes. Furthermore, it is applied in manufacturing thermal paper receipt^[1,2,3].

The greatest problematic route of human BPA exposure is the oral one via food consumption most probably due to leakage from canned food and beverages as well as through saliva from dental sealants and tooth coatings. The second most common route of BPA exposure is the transdermal absorption primarily through thermal paper handling. Additionally, BPA inhalation has been reported^[4].

BPA could be absorbed into the bloodstream and transferred to various tissues and organs. In the liver, it becomes strongly conjugated to create bisphenol A glucuronide, a significant metabolite which is excreted in urine^[5]. In human, BPA could be distinguished not only in the serum and urine but also in saliva and breast milk. Additionally, BAP was revealed in the tissue of placenta, amniotic fluid, maternal blood as well as in umbilical cord blood indicating that it can pass across the placental

barrier^[6,7]. Moreover, being one of the endocrine-disruptor compounds (EDCs), BPA could exhibit hormone-like properties. It is a xenoestrogen that can bind to estrogen receptors as an agonist meanwhile bind to androgen and thyroid hormone receptors but with antagonistic characteristics^[8]. Furthermore, BPA could enhance cancer susceptibility^[9].

Actually, EDCs have the ability to modify cardiovascular function, raising the need for research into their cardiotoxicity^[10]. Evidences from previous studies revealed that, BPA exposure gave rise to adipogenesis, obesity, hypertension, as well as various metabolic disorders^[11]. Also, it might be linked to insulin resistance, type 2 diabetes mellitus, as well as several cardiovascular diseases (CVDs)^[12].

Additionally, acute or prolonged BPA exposure has been associated with coronary, peripheral arterial, and CVDs. BPA could target intracellular Ca²⁺ promoting arrhythmia, accelerating atherosclerosis and inducing myocardial infarction, dilated cardiomyopathy, and hypertension^[13,14]. Furthermore, in BPA treated fish, calcified aortic valve disease, structural abnormalities, and extracellular matrix lesions have been reported^[15,16].

On the other hand, the majority of the aforementioned investigations have focused on the chemical and biological changes in the cardiovascular system (CVS) and few research^[17,18] has studied BPA impact on the histological cardiac construction. Additionally, scarce studies have been concerned with the possibility of spontaneous reversibility in the deleterious impact of BPA on various tissue organs. A recovery period for 4 weeks following daily oral BPA administration (50mg/kg/day) for 8 weeks displayed a marked improvement in the structure of all cell layers of the ductus epididymis^[19], as well as in the hepatic construction^[20] in adult male albino rats.

Up to our knowledge, there were no known earlier investigations regarding the curative outcome of recovery period on BPA induced myocardial histological alterations following BPA discontinuation. Due to the vast range of BPA applications, studies of BPA correlation to CVDs should be highlighted, especially with respect to the possible underlying mechanisms, prevention and treatment. So, the current study intends to clarify BPA induced cardiotoxicity, its reflection on various functional parameters in the adult rat heart, as well as to assess the possible reversibility following BPA cessation.

MATERIALS AND METHODS

Animals

The present study was carried out on healthy adult male Wistar albino rats [n=48, aged 20 weeks, weighing 220 ± 20 g]. The rats were purchased from Zagazig Scientific Medical and Researching Center's animal house (ZSMRC) which was the site of all animal experiments and sample collection. All through the study period, the animals were kept in specific stainless-steel cages (three rats / cage)

and were maintained in an air-conditioned room under environmentally typical laboratory settings [alternately, 12/12 periods of light and dark, a relative humidity of 50 ± 5% and a temperature of 23 ± 2 °C]. The rats were fed on standard laboratory rodent chow pellet besides water ad libitum. Prior to the start of any experimentation, a 14-day of acclimatization was permitted. All study protocols and animal husbandry were in accord with the Care and Use of Laboratory Animals' Guide, 8th edition^[21] and agreed with research protocols set by the Institutional Animal Care and Use Committee [IACUC], Zagazig University (ZU), Egypt, Approval number [ZU-IACUC/3/F/175/2022].

Chemicals

BPA powder (CAS Registry Number: 239658, Sigma), manufactured by Sigma-Aldrich company (St. Louis, MO, USA) and has been purchased from Sigma Egypt. The powder was freshly liquified in corn oil to be gavaged to non-anesthetized animals.

Experimental protocol

The rats under the present study were assigned at random as groups I, II, III and IV [n=12/group]. Group I (control negative): comprised animals that administered distilled water at a dose of 1mL. Group II (control positive): included animals that obtained corn oil at a dose of 1 mL. Group III (BPA group): involved animals that obtained BPA dosed 50 mg/kg body weight dissolved in 1mL corn oil^[19,20]. Throughout the previous treatments in groups I, II and III, a single freshly prepared daily dosage was administered orally by gavage for a total of eight weeks.

Group IV (recovery group): comprised animals that were administered BPA similar to group III; at the same dose and for the same duration, then left ad libitum without BPA administration for another four weeks before sacrifice.

Throughout the study, all rats were kept under constant observation for any mortality.

Experimental design

Blood and tissue collection

Just before sacrifice, an intraperitoneal injection of thiopental at a dose of 50 mg/kg body weight was used to induce general anesthesia in the rats at the end of each investigational period^[22]. Venous blood samples from the retro-orbital plexuses (3ml / rat in each study group) were obtained using capillary glass tubes. The sampled blood was left to clot at room temperature for 30 minutes. Then, the serum was separated via centrifugation for at least 15 minutes at 3000g and 4 °C. The detached serum was reserved at - 80 °C till used^[23]. The animals were then euthanized via decapitation. The following procedures were performed on each slain rat in each research group: the thoracic cavity was opened, the heart was quickly excised, and washed in an ice-cold saline solution. After that, the left ventricle was longitudinally dissected and split into 2 slices; one slice was cut into 5 mm³ pieces, fixed in 10% neutral-buffered formalin (pH = 7.4) for 24 h, and then

handled routinely to create paraffin blocks. These blocks were prepared through washing in 0.1 M phosphate buffer saline (SBS), dehydrating in ascending grades of alcohol, clearing, and then paraffin embedding. Afterwards, serially cut slices of 4–5 μm thick tissue were handled for histological and immune-histochemical analysis under a light microscope^[24]. On the other hand, 10% cardiac tissue homogenate was prepared by homogenizing the other left ventricular tissue slice in ice-cold isotonic saline using a homogenizer. After being centrifuged at 3000g for 10 minutes at 4 °C, the supernatant was collected and stored at – 80 °C Prior to further biochemical valuation.

Serum CK-MB estimation

Serum creatine kinase myocardial band (CK-MB) is a biomarker and a specific tool for evaluating cardiomyocyte injury. Quantitative measurement of the CK-MB activity was assessed spectrophotometrically via commercially available colorimetric kits (Bio-diagnostics, Giza, Egypt) as described by the producer.

Oxidative stress parameters evaluation

The supernatants from tissue homogenates were used to estimate myocardial content of both malondialdehyde (MDA) (lipid peroxidation end product) and reduced glutathione (GSH) levels. Additionally, they were applied to assess cardiac enzymatic activity of both Superoxide Dismutase (SOD) and Catalase (CAT). Commercially available colorimetric activity assay kits (Bio-diagnostics, Giza, Egypt) were utilized as described by the manufacturer.

Light microscopic studies

i. Evaluation of histological alterations, collagen and glycogen content, and mast cell density

Paraffin sections (4-5 μm thick) from each rat distinct groups were cut, dewaxed, rehydrated, slide mounted. Then, the slides were stained with H&E (Hematoxylin and Eosin) stain for cardiac tissue routine histopathological examination, MT (Masson's Trichrome) stain to demonstrate collagen fibers for assessment of cardiac fibrosis. Also, they were stained with PAS (Periodic acid Schiff's) stain to reveal glycogen deposition and with toluidine blue to quantitatively analyze the number of mast cells/ mm^2 . A LEICA research microscope (LEICA DM 500, Switzerland) with a digital camera (LEICA ICC50) was used to view the stained sections and obtain photomicrographs.

ii. Immunohistochemical staining for assessment of apoptosis, inflammation and fibroblast proliferation

Using duplicate 4-5 μm thick cardiac tissue slices, the paraffin-embedded tissue blocks of formalin-fixed left ventricular tissues were stained using immunohistochemistry. It was done via the avidin biotin peroxidase technique in accord with^[25]. For apoptosis assessment, a primary mouse monoclonal antibody (Cat: SC-7480, Santa Biotechnology, INC) against Bcl-2-associated X protein (Bax) was used at a dilution of

1:200. On the other hand, a rabbit polyclonal anti-rat antibody against the P65 subunit of nuclear factor kappa B (NF- κB), 1:20 dilution, ab86299, Abcam, Cambridge, Massachusetts, USA, was used to study NF- κB expression for inflammation evaluation. Furthermore, to demonstrate interstitial fibroblasts and endothelial cell lining of blood vessels in the cardiac tissue, the slices were incubated with anti-Vimentin (mouse monoclonal Vimentin antibody, Vim 3B4, Catalog No. M7020; Dakopatts CA, USA) at a dilution of 1:200. Briefly, 10 sections (4-5 μm thickness) /group were subjected to dewaxing in xylene, rehydration in graded ethanol solutions, bathing in tap water, preservation with 3% H_2O_2 for 10 minutes to block the endogenous peroxidase then immersion in antigen recovery solution. By soaking the sections in 10% normal serum of goat dissolved in phosphate buffer solution (PBS), common protein binding was prevented. After that, the sections were incubated with the primary anti-Bax, anti- NF- κB , or anti-Vimentin antibodies for a whole night at 4 °C. After washing in PBS, left ventricular slices received the corresponding biotinylated 2ry antibody for an hour at room temperature, followed by another PBS wash. For ten minutes, streptavidin peroxidase was added followed by washing again in PBS. After that, the chromogen 3, 3 diaminobenzidine (DAB) - H_2O_2 proved helpful for identifying the immunoreaction location. Mayer's hematoxylin was used as a counterstain on the immunostained heart slices. For slices served as negative control, the 1ry antibodies were omitted. Positive BAX-immunoreactivity was microscopically recognized through visualization of brown cytoplasmic discolored immunoreactive cells meanwhile it was a +ve brownish nuclear and/or peri-nuclear cytoplasmic immunoreactivity for NF- κB . Regarding Vimentin, the reaction was brownish cytoplasmic for fibroblasts, endothelium lining blood vessels and endomysium. A light microscope was used to visualize the slides.

Histomorphometry study

The image analyzing unit in the anatomy department, faculty of medicine, Zagazig university, Egypt, employed a Leica Qwin 500 image analyzing computer system for this investigation (Leica Microsystem Imaging Solution Ltd., Cambridge, UK) to determine the subsequent quantitative morphometry parameters in the distinct study groups. Quantitative assay of the mean area % for collagen fibers in MT stained slices and for glycogen content in PAS stained sections were estimated. Also, the mean area % of positive BAX; NF- κB and Vimentin immunoreactions in cardiac sections of all studied groups were assessed. Furthermore, the number of mast cells/ mm^2 was calculated. Measurements were obtained from 10 distinct non-overlapping randomly selected fields from each cardiac specimen in each rat of all groups under the study at ($\times 400$) magnification. Using Image-J® analysis software (NIH, USA), the mean value and standard deviation (SD) for each specimen was computed.

Statistical analysis

Graph Pad Prism 5.01 was used to computerize and statistically analyze the collected data for collagen, glycogen, mast cells/mm², BAX, NF- κ B and Vimentin. Quantitative data was shown as mean \pm SD (Standard deviation). Analysis of variance (ANOVA) was used to discover whether there were any significant differences between the experimental groups' mean values. Post hoc test of ANOVA; Tukey's multiple comparison test, was conducted when the *P* value <0.05 . The findings were considered statistically significant. Varying levels of significance were considered. When the *P* value <0.001 , it means high significance (***) while it becomes moderately significant (**) at $0.01 >P \text{ value} >0.001$ and low significant (*) if $0.05 >P \text{ value} >0.01$.

RESULTS

All rats under the study tolerated the entire experimental procedures and survived until the end of the investigation. Also, histological examination of sections obtained from both control negative and positive groups displayed no recognized structural differences. Similarly, both groups were within the same range with no significant differences between them regarding all studied morphometrical parameters ($P >0.05$). Therefore, the group I was selected to present the results of the group of control and was utilized in the statistical contrast versus other groups.

BPA induced histological alterations in rat's myocardium

BPA administration led to evident degenerative alterations in the rat myocardium signifying cardiotoxicity with a great improvement following BPA withdrawal. Using light microscope, H&E stained sections from left ventricular tissue of control group, exhibited typical histological construction; formed of branching and anastomosing cardiac muscle fibers with single ovoid centrally placed vesicular nuclei and acidophilic sarcoplasm. Additionally, fibroblasts (had darkly stained flattened nuclei) and blood capillaries were distinguished in the connective tissue (CT) gaps between heart muscle fibers (Figure 1a).

Relative to the control group, sections gained from BPA-administered rats (group III), demonstrated significant degenerative abnormalities manifested as discontinuation, wide separation, and the disarray of cardiac muscle fibers. Some cardiomyocytes appeared shrunken and exhibited deeply stained homogenous acidophilic sarcoplasm and pyknotic nuclei while others presented perinuclear sarcoplasmic vacuolation. Also, dilated congested capillaries were well demonstrated (Figures 1b,c) and some vessels displayed thick vacuolated walls (Figure 1d).

Additionally, the CT cell proliferation was well recognized both perivascular (Figure 1e) and interstitial (Figure 1f). Furthermore, extensive hemorrhage (Figure 1g) and RBCs extravasation (Figure 1h) were exhibited amongst cardiac muscle fibers meanwhile

foci of mononuclear inflammatory cell infiltrate were demonstrated between cardiomyocytes (Figure 1i) and in proximity to blood vessels (Figure 1j).

Interestingly, sections taken from animals in the recovery group (group IV) presented a great improvement in the heart structure and became more or less identical to the control group. Most cardiomyocytes appeared normal and displayed acidophilic sarcoplasm, and oval centrally located vesicular nuclei. Nevertheless, some cells were still showing perinuclear vacuolations. Besides, mild inflammatory cell infiltration, and vascular congestion were still exhibited (Figures 1k,l).

BPA led to increased myocardial fibrous tissue content

The widely separated cardiac muscle fibres seen in H&E-stained sections from BPA-treated rats (group III) would be the consequence of the replacement of the injured contractile muscle fibers with fibrous structures. Therefore, sections were stained with the collagen-specific dye, Masson's trichrome (MT), and were examined using light microscope to better support this suggestion.

A minor amount of green coloured collagen fibres was dispersed in the connective tissue (CT) gaps separating cardiac muscle fibers and also surrounding the blood vessels in sections of the control group (Figure 2a). In contrast, cardiac sections from rats that had received BPA demonstrated the greatly increased amount of collagen (Figure 2b). On the other hand, after BPA withdrawal for 4 weeks in the recovery group (group IV), comparable to group III, an evident improvement was manifested as a marked reduction in the amount of collagen fibre deposition to be relatively similar to the group serving as the control (Figure 2c). These findings were further confirmed by quantification of the collagen area percentage that established a high substantial rise in the mean area % occupied by collagen in BPA-treated group (group III) proportional to the group of control (5.847 ± 1.461 and 0.621 ± 0.110 , respectively, mean \pm SD, $P < 0.0001$). However, in recovery group (group IV), BPA withdrawal resulted in a highly substantial reduction in mean area % occupied by collagen compared to BPA-treated group (group III) (1.515 ± 0.288 and 5.847 ± 1.461 respectively, mean \pm SD, $P < 0.0001$). Fortunately, there was a non-significant difference between the recovery and control groups ($P >0.05$) (Figure 2d, Table 1).

BPA led to increased glycogen content of cardiomyocytes

Regarding the glycogen distribution in the cardiac muscle fibers determined via PAS stain, sections from rats in the control group displayed a minimal amount of glycogen content (Figure 3a). However, the amount of glycogen was obviously increased in BPA-receiving group (group III) respect to the control one (Figure 3b). BPA withdrawal in the recovery group (group IV), seemed to decrease the amount of glycogen deposited compared to

BPA-treated group but still more than that in the group of control (Figure 3c). Additionally, these findings were further confirmed by quantification of the glycogen area percentage that demonstrated a high substantial rise in the mean area % occupied by glycogen in BPA-treated group (group III) in comparison to the group of control (12.250 ± 1.340 and 2.594 ± 0.928 respectively, mean \pm SD, $P < 0.0001$). However, regarding recovery group (group IV), contrasted to BPA-treated rats (group III), BPA withdrawal experienced a high significantly decreased mean value (4.541 ± 1.013 and 12.250 ± 1.340 respectively, mean \pm SD, $P < 0.0001$). Nevertheless, there was only a low statistically significant difference between the recovery and control groups ($0.05 > P > 0.01$). (Figure 3d, Table 1).

BPA induced increased mast cell number in rat's myocardium

To determine the potential influence of BPA administration on the heart's mast cells, left ventricular tissue sections from study groups were stained using toluidine blue. Mast cells were distinguished (large violet stained cells in a blue background because of their content of metachromatic cytoplasmic granules) in slices from rats in all experimental groups. Regarding the control group, fewer mast cells were displayed (Figure 4a) meanwhile the BPA-treated group exhibited obviously an increased mast cell number (Figure 4b). The recovery group showed mast cells that appeared moderate in number (Figure 4c). Furthermore, the morphometrical and statistical analysis confirmed the previous findings and demonstrated a significant rise in the mean number of mast cells per mm^2 in the BPA-treated group (group III) as compared with the control group (62.499 ± 16.106 and 17.578 ± 6.176 , respectively, mean \pm SD, $P < 0.0001$). However, the recovery group's mean number of mast cells per mm^2 was considerably lower compared to the BPA-treated group, (group III) (29.297 ± 8.735 and 62.499 ± 16.106 respectively, mean \pm SD, $P < 0.0001$). However, the difference between the recovery and control groups was hardly significant ($0.05 > P > 0.01$) (Figure 4d, Table 1).

BPA induced immunohistochemical alterations in rat's myocardium Immunohistochemistry and Morphometry for BAX

Bax immunostained heart sections displayed a limited positive brown sarcoplasmic reaction in few cardiomyocytes in the control group (Figure 5a) while it was strong and widely distributed in most cardiomyocytes in BPA-treated group (group III) (Figure 5b). Fortunately, a marked improvement occurred in the recovery group (group IV) so the reaction appeared mild to moderate and included some cardiomyocytes (Figure 5c). These findings were further established by morphometrical quantification of Bax immune-expression area %, and a statistical analysis was performed for comparison among groups. The mean area % of Bax immune-expression in BPA-treated group (group III) was highly significantly increased ($11.042 \pm$

3.721) contrasted with the control group (0.127 ± 0.002) meanwhile, it was highly significantly decreased (1.317 ± 0.275) in the recovery group (group IV), as compared to the BPA receiving group. Fortunately, non-significant difference regarding control versus recovery groups was found ($P > 0.05$) (Figure 5d, Table 1).

Immunohistochemistry and Morphometry for NF- κ B

Left ventricular sections immunostained with anti-NF- κ B displayed a positive brown nuclear and/or perinuclear cytoplasmic immune-reaction only in few cardiomyocytes in the control group (Figure 6a). The reaction was apparently strong and widely distributed in most cardiomyocytes in BPA-receiving group (group III) (Figure 6b). However, it was declined in the recovery group (group IV) (Figure 6c). The previous findings were confirmed via morphometrical quantification of NF- κ B immune-expression area %, and a statistical analysis was performed for comparison between groups. The mean area% of NF- κ B immune expression increased significantly in the group that received BPA (4.325 ± 1.095) contrasted with the control group (0.582 ± 0.137), meanwhile the mean area% of NF- κ B immune expression decreased significantly (1.715 ± 0.876) in the recovery group compared to the BPA-receiving group. However, low significant difference between control and recovery groups was recognised ($0.05 > P > 0.01$) (Figure 6d, Table 1).

Immunohistochemistry and Morphometry for Vimentin

Additionally, by using the Vimentin immunostaining method, it was possible to see interstitial fibroblasts, vascular endothelial lining, and endomysium of the control group's heart sections that had only minor Vimentin immunoexpressing (Figure 7a). However, sections of rats that only received BPA showed enhanced Vimentin expression (Figure 7b) as opposed to reduced expression in the recovery group (Figure 7c). These findings were further confirmed by quantification of the Vimentin area percentage that exhibited a highly significant rise in the mean area % occupied by Vimentin in the BPA-treated group (group III) comparable to the group of control (5.850 ± 1.67 and 1.294 ± 0.264 respectively, mean \pm SD, $P < 0.0001$). However, regarding the recovery group (group IV), contrasted to BPA-treated rats, BPA withdrawal experienced a low instead of high significantly decreased mean value (group III) (2.421 ± 0.52 and 5.850 ± 1.67 respectively, mean \pm SD, $P < 0.0001$). Yet, there was a low significant difference between recovery and control groups ($0.05 > P > 0.01$) (Figure 7d, Table 1).

BPA induced significant alterations in the biochemical parameters

The BPA-treated animals (group III) displayed a significantly highly increased mean value of MDA (3.65 ± 0.079 nmol/mg) and CK-MB (986 ± 37.42 U/L) levels in contrast to the control group (0.89 ± 0.029 nmol/mg, 421.2 ± 13.2 U/L respectively) ($p < 0.001$). On the

other hand, BPA withdrawal in the recovery group resulted in regression in the mean values of MDA (1.581 ± 0.054 nmol/mg) and CK-MB (598 ± 26.04 U/L) but still showing low significant differences versus control group ($0.05 > p > 0.01$). Furthermore, BPA treatment resulted in a highly significant decline in GSH level (33.78 ± 2.79 ng/mg), SOD (63.32 ± 3.32 U/mg), and CAT (3.43 ± 0.53 ng/mg)

activities contrasted to the control group (91.38 ± 3.14 ng/mg, 118.17 ± 3.17 U/mg, 7.12 ± 0.66 U/mg respectively) ($p < 0.001$). However, following the BPA withdrawal in the recovery group, their values were increased (69.93 ± 4.17 ng/mg; 97.93 ± 4.15 U/g; 5.92 ± 0.71 ng/mg respectively) but still presenting low significant difference comparable to the control group ($0.01 < p < 0.05$) (Table 2).

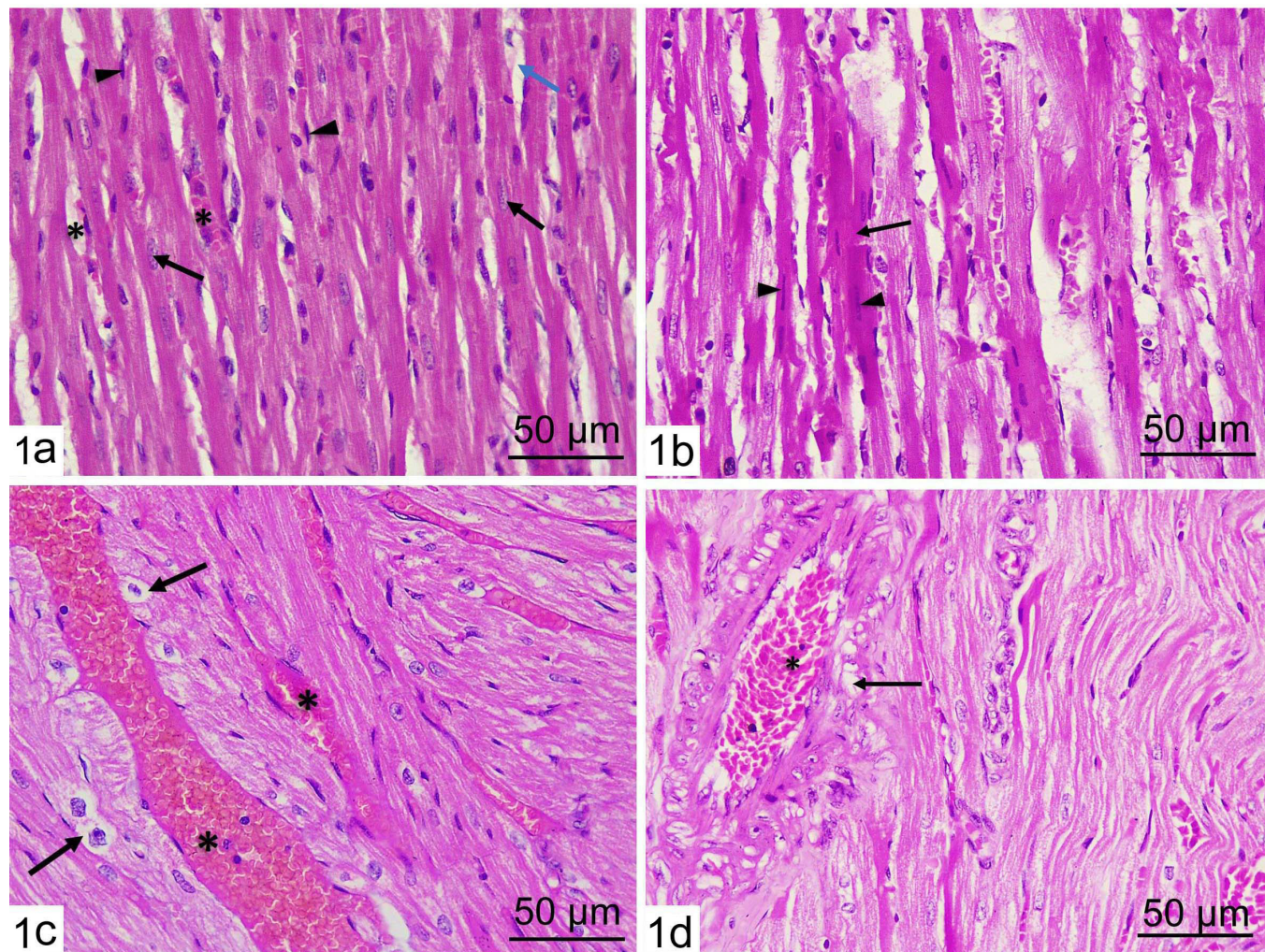


Fig. 1A: Representative photomicrographs of longitudinal sections of left ventricular myocardium of the control group (a) and BPA treated group (b,c,d) demonstrating [a]: branching and anastomosing cardiac muscle fibers, centrally placed ovoid vesicular nuclei (black arrow), and interstitial CT spaces (blue arrow) containing blood capillaries (*) and fibroblasts with flat dark nuclei (arrowhead). [b]: cardiac muscle fibers exhibiting discontinuation, wide separation, dark acidophilic sarcoplasm (arrow) and pyknotic nuclei (arrowhead). [c]: cardiomyocytes exhibiting disarray, perinuclear sarcoplasmic vacuolation (arrow) with dilated congested capillaries in-between (*). [d]: the blood vessel (*) exhibiting thick vacuolated wall (arrow). (H&E× 400)

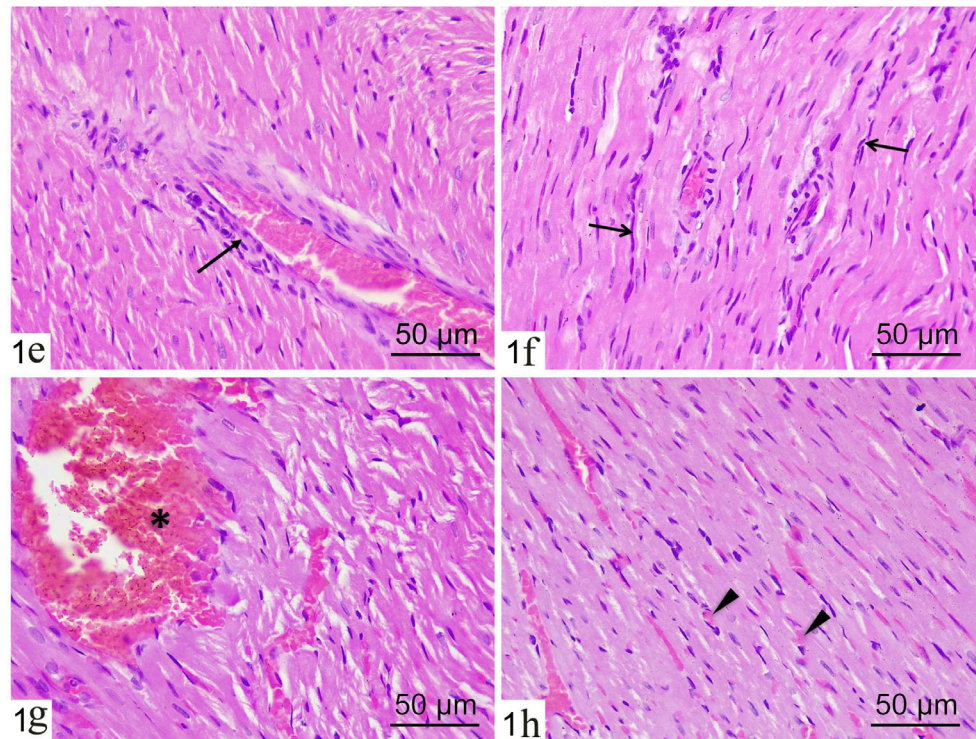


Fig. 1B: Representative photomicrographs of longitudinal sections of left ventricular myocardium of BPA treated group (e,f,g,h) showing [e]: perivascular CT cell proliferation (arrow). [f]: interstitial CT cell proliferation (arrow) [g]: extensive hemorrhage (*) among cardiomyocytes. [h]: excess RBCs extravasation (arrowhead) between cardiac muscle fibres. (H&E×400)

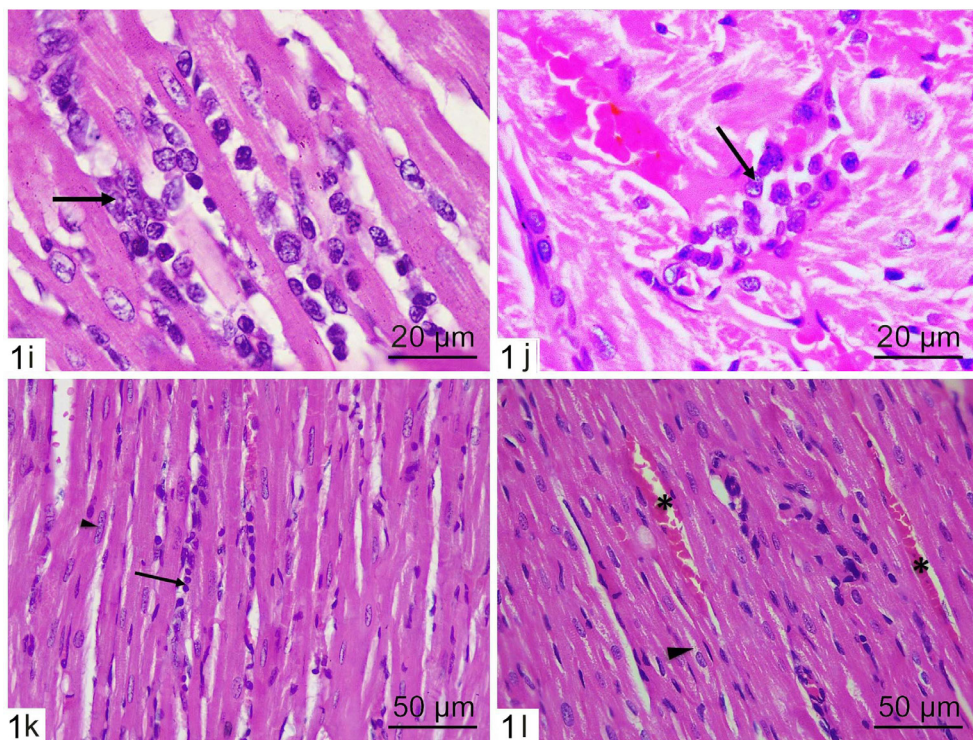


Fig. 1C: Representative photomicrographs of longitudinal sections of left ventricular myocardium of BPA treated group (i,j) and recovery group (k,l) showing [i]: mononuclear cellular infiltration (arrow) between cardiomyocytes. [j]: mononuclear inflammatory cell infiltrate (arrow) in proximity to blood vessels. [k]: mild cellular infiltration (arrow) between apparently normal cardiomyocytes with centrally located oval vesicular nuclei (arrowhead). [l]: some mildly dilated congested (*) capillaries and few cardiomyocytes with perinuclear vacuolation (arrowhead). (i,j H&E×1000 - k,l H&E×400)

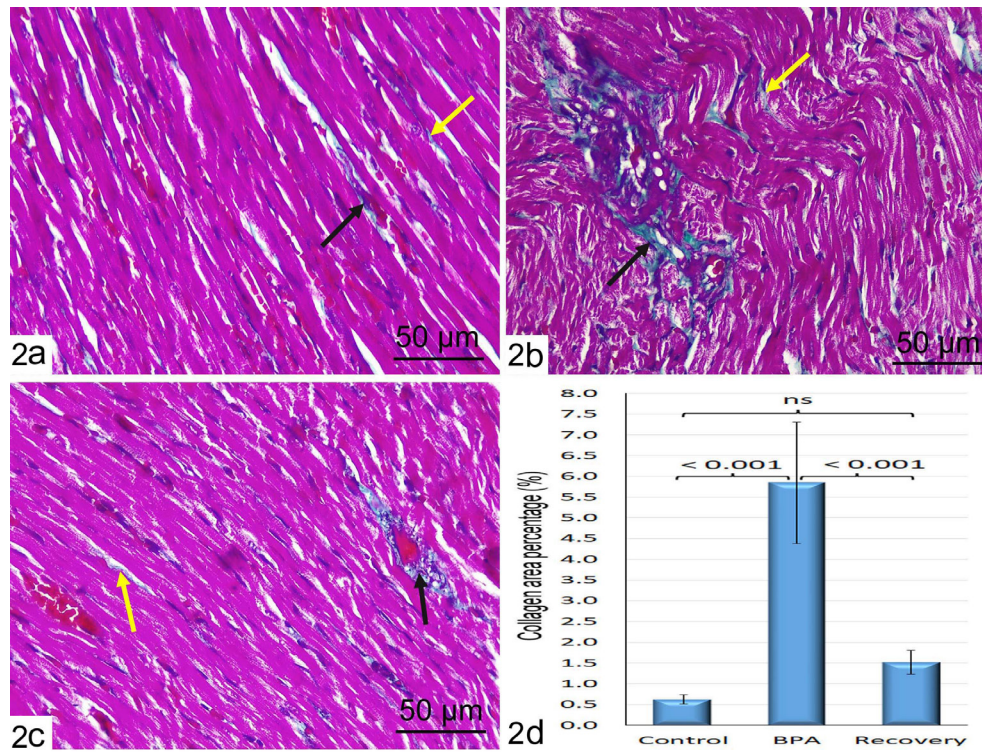


Fig. 2: Representative photomicrographs of longitudinal sections of left ventricular myocardium stained with MT demonstrating green colored collagen fibers in the CT spaces between cardiomyocytes (yellow arrow) and around the blood vessels (dark arrow) [a]: demonstrates delicate collagen fibers in the control group. [b]: exhibits an increased amount of collagen fibers in BPA-treated group. [c]: displays less amount of collagen fibers in the recovery group. (MT stain $\times 400$). [d]: Bar charts demonstrating the quantitative analysis of collagen fibers area % of the studied groups. Data are presented as mean \pm SD. ns: Non-significant

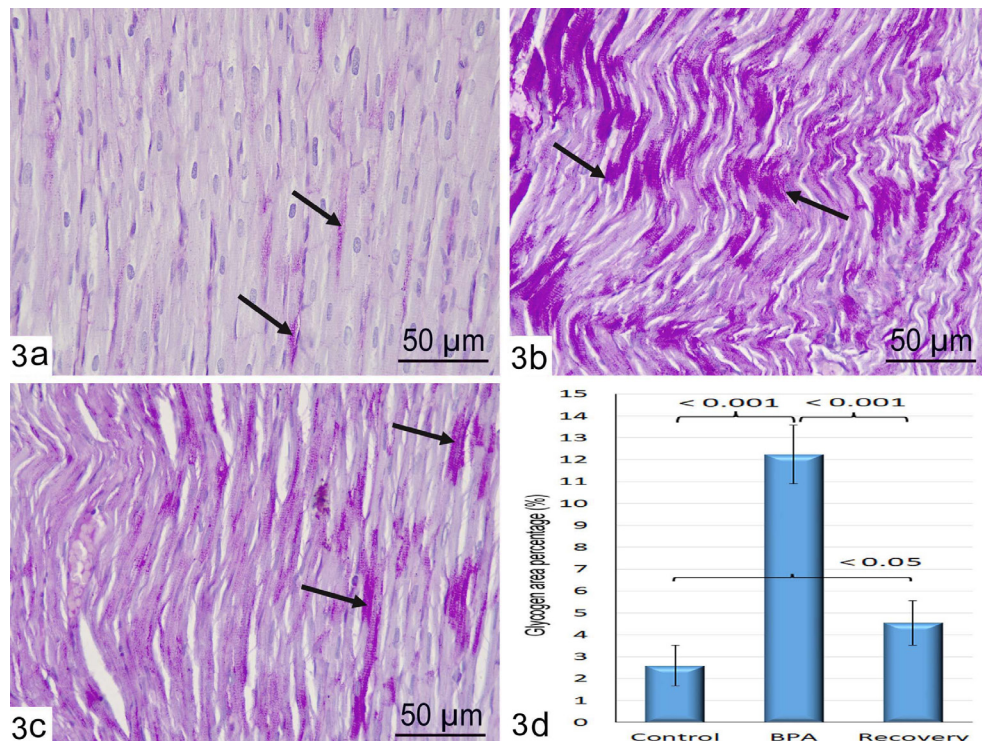


Fig. 3: Representative photomicrographs of longitudinal sections of left ventricular myocardium stained with PAS displaying glycogen content manifest as magenta coloration (arrow). [a]: a little glycogen content in the control group. [b]: a marked increase in the glycogen content in BPA-treated group apparent as diffuse dark magenta coloration. [c]: a moderate amount of glycogen content in the recovery group. (PAS stain $\times 400$). [d]: Bar charts demonstrating the quantitative analysis of area % of glycogen content of cardiac muscle fibers in the experimental groups. Data are presented as mean \pm SD.

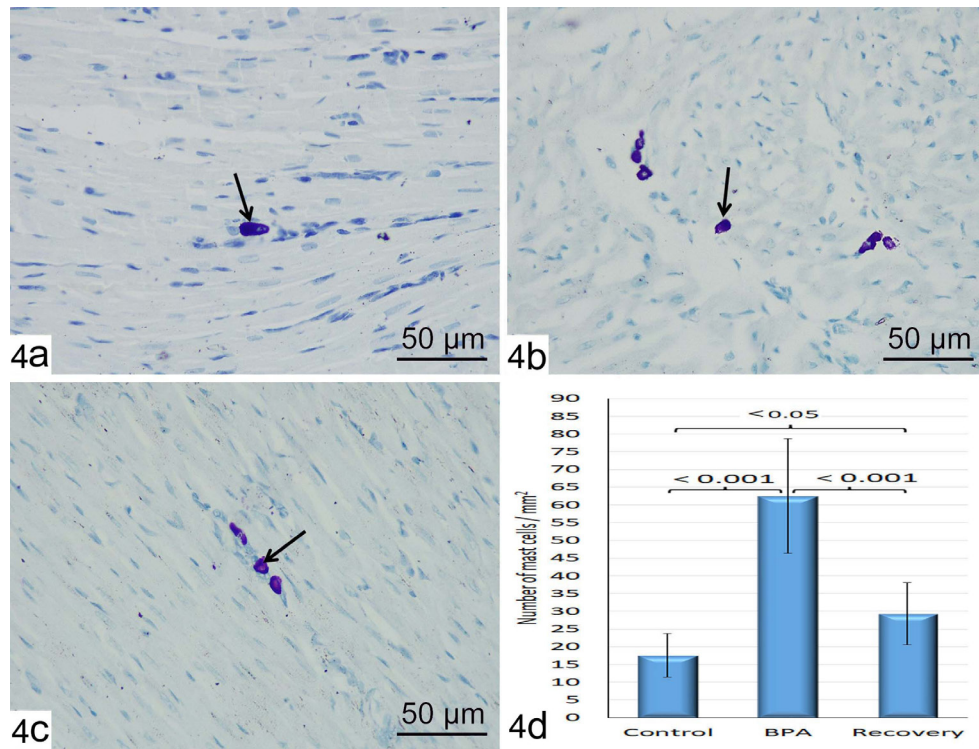


Fig. 4: Representative photomicrographs of longitudinal sections of left ventricular myocardium stained with toluidine blue demonstrating mast cell (arrow) density. [a]: the control group displays few mast cells. [b]: BPA-treated group exhibits obviously increased mast cell number. [c]: the recovery group shows mast cells that appear moderate in number. (Toluidine blue stain $\times 400$). [d]: Bar charts demonstrating the quantitative measurements of density of mast cells (number/mm²) among all studied groups. Data are presented as mean \pm SD.

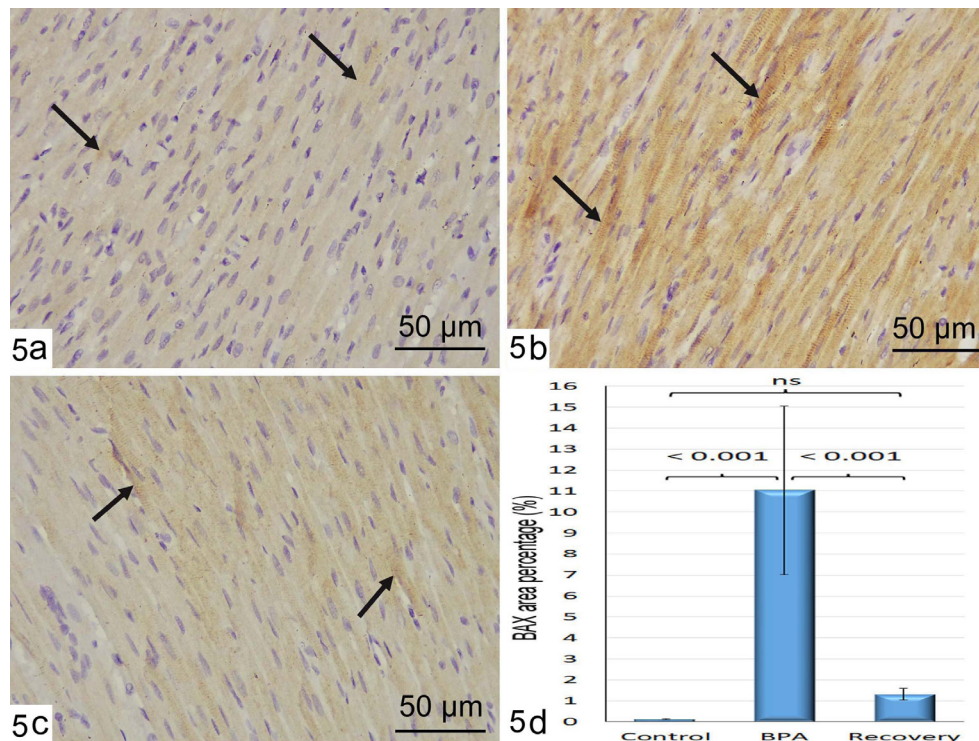


Fig. 5: Representative photomicrographs of immunohistochemically stained left ventricular sections with anti-BAX antibody demonstrating a positive brown cytoplasmic immunoreaction for BAX (arrow); in few cardiomyocytes in the control group [a], in many cardiomyocytes in the BPA- treated group [b], in some cardiomyocytes in the recovery group [c]. (anti-BAX immunostaining $\times 400$). [d]: Bar charts presented quantitative analysis of the area % of anti-BAX immunostaining in the distinct experimental groups. Data are presented as mean \pm SD. ns: Non-significant

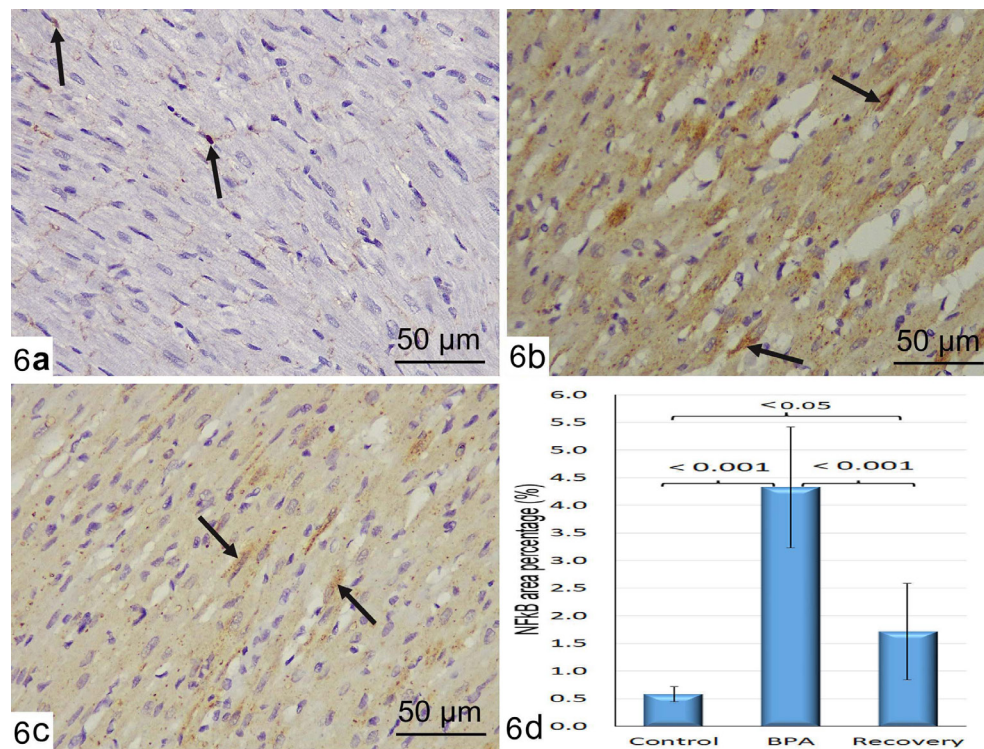


Fig. 6: Representative photomicrographs of immunohistochemically stained left ventricular sections with anti-NF-κB antibody demonstrating a positive brown nuclear and/or perinuclear immunoreaction for NF-κB (arrow); in few cardiomyocytes in the control group [a], in many cardiac cells in the BPA- treated group [b], in some cardiomyocytes in the recovery group [c]. (anti- NF-κB immunostaining ×400). [d]: Bar charts present quantitative analysis of the area % of anti-NF-κB immunostaining in the distinct experimental groups. Data are presented as mean ± SD.

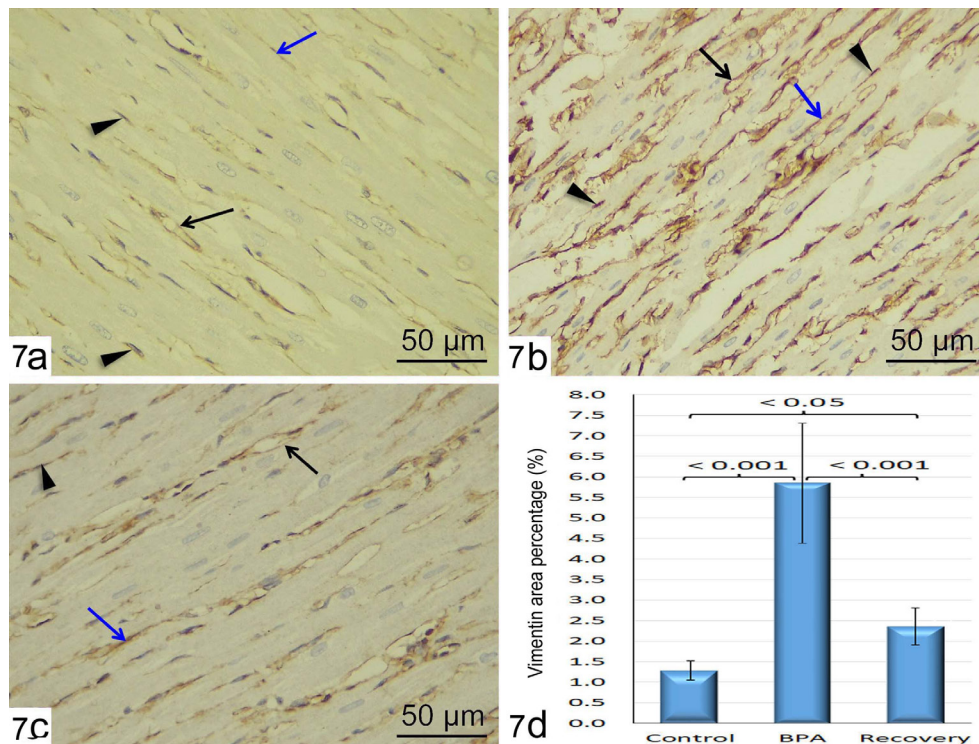


Fig. 7: Representative photomicrographs of immunohistochemically stained left ventricular sections with anti-Vimentin antibody demonstrating a minimal positive brown cytoplasmic immunoreaction in the interstitial fibroblasts (arrowhead), endothelial lining of blood capillaries (black arrow) and endomysium (blue arrow) seen in a section from control group [a]. However, a section obtained from BPA-treated group [b] shows moderate Vimentin immunoexpressing while section taken from recovery group [c] demonstrates a mild immune reaction. (anti-Vimentin immunostaining ×400). [d]: Bar charts present quantitative analysis of the area % of anti-Vimentin immunostaining in the distinct experimental groups. Data are presented as mean ± SD.

Table 1: Mean \pm SD of area % of collagen, glycogen, BAX, NF-k β , Vimentin, and mean \pm SD of mast cell number /mm²

Parameter	Control Mean \pm SD	BPA Mean \pm SD	Recovery Mean \pm SD	ANOVA	Tukey's Post hoc test		
					Control Vs BPA	Control Vs Recovery	BPA Vs Recovery
Collagen (%)	0.621 \pm 0.110	5.847 \pm 1.461	1.515 \pm 0.288	< 0.0001	***	ns	***
Glycogen (%)	2.594 \pm 0.928	1.340 12.250 \pm	1.013 4.541 \pm	< 0.0001	***	*	***
BAX (%)	0.127 \pm 0.002	11.042 \pm 3.721	1.317 \pm 0.275	< 0.0001	***	ns	***
NF-k β (%)	0.582 \pm 0.137	4.325 \pm 1.095	1.715 \pm 0.876	< 0.0001	***	*	***
Vimentin (%)	1.294 \pm 0.264	5.850 \pm 1.67	2.421 \pm 0.52	< 0.0001	***	*	*
Mast cells/mm ²	17.578 \pm 6.176	62.499 \pm 16.11	29.297 \pm 8.735	< 0.0001	***	*	***

High significance (***) means P value < 0.001, Moderate significant (**) at 0.01 > P value > 0.001 and low significance (*) when 0.05 > P value > 0.01.

Table 2: Mean \pm SD of laboratory parameters (MDA, CK-MB, GSH, SOD, and CAT).

Groups	CAT (ng/mg)	SOD(U/mg)	GSH (ng/mg)	CK-MB(U/L)	MDA (nmol/mg)
Control	7.12 \pm 0.66	118.17 \pm 3.17	91.38 \pm 3.14	421.2 \pm 13.2	0.89 \pm 0.029
BPA-treated	3.43 \pm 0.53 ***	63.32 \pm 3.32 ***	33.78 \pm 2.79 ***	986 \pm 37.42***	3.65 \pm 0.079 ***
Recovery	5.92 \pm 0.71*	97.93 \pm 4.15*	69.93 \pm 4.17*	598 \pm 26.04*	1.581 \pm 0.054*

Data are presented as means \pm SD. * p < 0.05 and *** p < 0.001 with Low (*) and high significance (***) P value vs control

DISCUSSION

The findings of the current study demonstrated manifest disturbances in the cardiac tissue construction including vascular congestion, hemorrhage, RBCs extravasation, cell infiltration, cardiomyocyte's vacuolation and pyknosis, associated with numerous signs of fibrosis, apoptosis and inflammation. Such results were in line with other animal reports that have described parallel structural changes in the rat myocardium as a response to either low BPA doses^[17], high doses^[26], or over a lengthy period of time^[27].

The deeply stained homogenous acidophilic (hyper-eosinophilic) sarcoplasm of many cardiomyocytes displayed in the current work agrees with^[17]. Also, similar findings were reported in association with other cardiotoxic compounds such as cyclophosphamide^[28], gentamycin^[29] and Doxorubicin^[30]. This hyper-eosinophilia might be attributed to the increased binding of eosin to degraded cytoplasmic proteins. This increased protein degradation might be in part due to the hydrolytic enzymes released from lysosomes in dying and dead cells^[31,32]. The cardiomyocyte perinuclear sarcoplasmic vacuolation encountered in the current work might be due to distended T-tubules and sarcoplasmic reticulum according to^[33].

In this work, cardiomyocyte deeply stained pyknotic nuclei were in parallel with^[34] who proposed that, BPA could induce oxidizing stress, excess ROS production, DNA breakdown, apoptosis and/or inflammation with the subsequent disintegration of structural proteins in both mitochondria and cell membranes. Additionally, the previous authors outlined the so-called ROS-induced ROS release phenomenon, as a contributing factor in which, excessively released mitochondrial ROS could induce ROS production in neighboring mitochondria, with subsequent

ROS overproduction. Cardiovascular cells would be affected by this mitochondrial crosstalk, which results in apoptosis, necrosis, and even fibrosis.

In the current study, vascular disorders, such as congestion, dilatation, RBCs extravasation, hemorrhage, as well as vacuolation and thickening in blood vessel walls were well demonstrated. These findings confirmed the results of previous investigators who emphasized that, BPA exposure is associated with a high risk of developing coronary as well as peripheral arterial disorders^[35,36].

Vascular congestion and dilatation encountered in the present study were interpreted by^[37] who attributed them to the enhanced release of endothelial nitric oxide synthase (eNOS) with resultant excess Nitric Oxide (NO) liberation next to BPA exposure. Actually, eNOS could normally preserve *in vivo* cardiovascular integrity by generating NO which promotes vasodilation, and possesses several antiatherogenic properties.

RBCs extravasation and hemorrhage displayed in current work were in accord with^[38] who interpreted them to be due to the weakened blood vessel wall carried out by inflammation, endothelial cell detachment, vascular leakage, and interstitial hemorrhage. Additionally, the thick-walled, vacuolated blood vessels revealed in this study agreed with^[18], who specified similar changes in the dorsal aorta's wall following BPA administration and attributed them to atherosclerotic changes.

Klint *et al*^[37] and Dabravolski *et al.*^[39] clarified BPA-induced atherosclerotic changes to be due to excess vascular endothelial growth factor (VEGF) generation, an angiogenic agent facilitating and regulating angiogenesis. Actually, the augmented VEGF signaling would increase

angiogenesis contributing to the development of atherosclerosis by facilitating the formation and rupture of atherosclerotic plaques.

The interstitial mononuclear cell infiltration demonstrated in this study agreed with^[40] who ascribed it to be due to BPA- induced excess ROS release with consequent triggering inflammation reactions and leukocytes immigration into the injured cardiomyocytes.

In this work, multiple signals were suggestive of BPA-induced excess myocardial fibrosis manifested as increased CT cells both perivascular and interstitial in H&E stained sections; considerable high degree of collagen fibre deposition demonstrated in MT stained slices, besides the highly significantly raised area % of Vimentin positive immunological reaction. These results closely matched^[41,42] who attributed the augmented myocardial fibrosis to be due to increased fibroblast proliferation with subsequent excess collagen synthesis.

Actually, fibroblasts are dormant cells in the healthy heart that simply maintain the extracellular matrix's balance (ECM). They have a significant role in cardiac remodeling in the sick myocardium like proliferation, migration, and enhanced ECM turnover producing a significant amount of interstitial collagen^[43].

Additionally, cardiac mast cells' raised density and/or activation could be a contributing factor to myocardial fibrosis through both direct and indirect impacts on fibroblasts. Mast cells can produce numerous proteases, cytokines, growth factors, and others^[44]. Besides, excessive interstitial fibrosis may be brought on by activation of the NF-B transcription factor^[45]. Also, a molecular mechanism linking cardiac fibrosis with oxidative stress, nutrition, and inflammation was outlined^[46]. Furthermore, both cardiovascular and central nervous systems simultaneously experienced detrimental structural remodeling as a result of oxidative stress^[47].

In the present investigation, the mean area percentage of Vimentin-positive immunoreaction increased significantly in the BPA-treated rats compared to the control group. These findings agreed with^[26]. It was proposed that, Vimentin and other cytoskeletal protein deviations during cardiac pathology and failure could affect intracellular signaling, cardiomyocyte function, as well as cardiomyocyte coupling to the ECM^[48]. In addition, the cardiac cytoskeleton keeps the cellular organelles organized internally. Also, it transfers intracellular mechanical stresses to neighboring cells and ECM^[49]. Furthermore, changes in intracellular calcium concentrations could be a contributing factor for the altered Vimentin immunoexpressing^[50].

The results of the current study displayed a significantly higher mean number of mast cells per mm², in BPA-receiving group than that in the other experimental groups. This agrees with^[51] who previously reported that, perinatal BPA exposure enhanced the activity of mast cells in adulthood which in turn increased the generation of pro-inflammatory mediators linked to asthma.

Ingason *et al.*^[52] added that, mast cell derived-chymase has been associated with a number of cardiovascular illnesses, including atherosclerosis, arrhythmias, myocardial ischemia, heart failure, and ventricular hypertrophy.

Contrary to our findings,^[17] examined the BPA impact (dosed 1.2 mg/kg obtained daily via the intraperitoneal route for three weeks) on the rat myocardium and reported non-significant differences in mast cell number of per mm² amongst the trial groups despite excess myocardial fibrous tissue and collagen content. However, this would be attributed to the lesser dose and the shorter time of BPA exposure comparable to that in our study.

In this study, glycogen accumulation in cardiomyocytes of BPA-treated group was well demonstrated using PAS stain, meanwhile the heart sections of control animals showed a minimal amount. Similar findings were reported in methotrexate- induced cardiotoxicity whereas PAS positive reaction was increased in the perinuclear area of cardiomyocytes, and was attributed to the presence of perinuclear vacuolation^[53]. Also, mitochondrial disorder of cardiac muscles has been a leading factor in glycogen accumulation in the perinuclear region of cardiomyocytes because of free radicals' accumulation^[54].

Furthermore, after sub-chronic treatment with the mitochondrial toxin 3-nitropropionic acid (3NPA), researchers examined the glycogen content of rat myocardium and displayed a significant accumulation of glycogen granules in 3NPA-treated rats meanwhile the control animals' hearts had almost no glycogen granules. Actually, animal cells could use glycogen as a secondary kind of long-term energy storage. Also, both glycogen synthase and glycogen phosphorylase enzymes could regulate glycogen production and breakdown respectively. Regulation of both enzymes is very complicated and is influenced by a variety of variables^[55].

In our study, although the mechanism and the pathophysiological implications of BPA induced glycogen accumulation in cardiomyocytes are currently unclear, this finding offers an interesting starting point for additional research.

Many investigators have suggested that, in spite of lacking macroscopic cardiac injury, low BPA doses have been associated with manifest changes in the heart structure assessed by liquid chromatography mass spectrometry (LC-MS/MS) as well as via infrared spectroscopy. Additionally, low BPA doses have been associated with gene expression variations, carrying a risk of disease load^[56].

According to this study's immunohistochemistry results, rats treated with BPA had significantly raised levels of the mitochondrial-dependent apoptosis pathway regulator (BAX), as well as the primary inflammatory mediator (NF-κB) in the cardiac tissue. In support of these findings in our study, we detected a considerable decline in their immune-expression levels manifested both

histologically and by quantitative morphometric methods after 4-weeks recovery.

Similar to our findings, in other animal investigations, BPA augmented BAX immunohistochemistry expression in the cardiac tissue^[57], in whole cell layers of the ductus epididymis^[19] as well as in the hepatocytes^[20].

As a mammalian endocrine disruptor, BPA contributes to the production of a number of proinflammatory cytokines such as IL-1, IL-6, and TNF α . Additionally, proinflammatory mediators like NO and PGE2 as well as their upstream regulators (iNOS; COX2; cPLA2) were found to express themselves more often in response to BPA. Furthermore, according to reports, BPA may cause the NF- κ B signaling pathway to be upregulated and dramatically increase the phosphorylation and nuclear translocation of NF- κ B p65 via I κ B degradation^[58].

It was emphasized that, NF- κ B-mediated inflammation is one of the primary mechanisms of CVDs. Cytokines, chemokines as well as adhesion molecules such as IL-6, MCP-1, and VCAM are produced by means of NF- κ B activation. Additionally, NF- κ B contributes to inflammasomes' control and stimulates pro-inflammatory gene expression including those encoding cytokines and chemokines. Furthermore, NF- κ B is crucial for innate immune cell regulation, as well as inflammatory T-cells, survival, activation, and differentiation. Consequently, uncontrolled NF- κ B activation may have a role in the pathogenesis of numerous inflammatory illnesses^[59,60,61].

The results of the present study showed that, BPA administration significantly increased both CK-MB activity and MDA level compared to control values and significantly decreased SOD, CAT, and GSH levels below control values. The previous findings indicated cardiac tissue injury and inflammation which might be due to a state of oxidative stress in the rat cardiomyocytes. These findings were in line with^[62] who stated that, BPA administered in a dose of 50 mg/kg/day for 4 weeks had a negative impact on the heart due to elevation of both CK-MB activity and MDA level while dropping GSH level.

Also, our findings were in accord with^[63] who proved that, BPA significantly impaired the construction and function of many vital organs; the kidney, liver, testes, and pancreas, in animal models via raising BPA's production of ROS. The previous authors added that, BPA could alter the balance of enzymatic antioxidants by lowering SOD, GSH, and CAT levels in both blood and pancreas of BPA-exposed animals.

It was concluded that, several mechanisms have been implicated with BPA cardiotoxicity. BPA exposure enhances oxidative stress via inducing the generation of oxygen radicals, significantly increasing ROS release, disturbing the dynamic balance of antioxidative enzymes, with subsequent ROS -antioxidizing defense imbalance, leading to cell and tissue damage, and homeostatic failure. Also, DNA, proteins in cells, lipids in cell membranes,

calcium influx, and mitochondria, all can be harmed. Actually, Superoxide dismutase (SOD), Catalase, and Glutathione S-transferase (GST), all are examples of enzymatic antioxidants that can scavenge and neutralize free radicals, and restore cellular integrity. Hydroperoxides, hydrogen peroxide (H₂O₂), and the superoxide radical, all could be converted into oxygen, water, and harmless molecules, respectively^[63].

Additionally,^[64,65] reported that, the excessively generated ROS can mediate many inflammatory responses via activation of not only NF- κ B but also numerous inflammatory mediators. Furthermore, being a metabolic and an endocrine disruptor, BPA could interfere with redox homeostasis by increasing oxidative mediators meanwhile decreasing antioxidant enzymes, resulting in mitochondrial malfunction, alterations in cell signaling pathways, and activation of cell apoptosis and death.

Furthermore,^[66] revealed that, BPA could impair cardiac excitability via various intracellular mechanisms such as inhibition of chief ion channels, disparities in Ca²⁺ handling, initiation of oxidative stress, and epigenetic alterations.

In controversy to our findings in this study,^[67] stated that, neonatal mouse ovarian cells exposed to BPA in utero or *in vitro* displayed no appreciable changes in SOD level. This was attributed to the small BPA dosage used (50 μ g/kg body weight) which might be insufficient to cause mice's antioxidant defense to weaken or not to develop at all.

Interestingly, in the current study, the recovery and reversibility of cardiac cells following the cessation of BPA administration were examined. After 4 weeks of BPA stoppage, it was clear that, the majority of the evaluated study parameters had greatly improved. The cardiac tissue has largely returned to normal conditions with only a minor degree of pathology, including perinuclear vacuolation of some cardiomyocytes accompanied with remaining small grade of congestion as well as mild inflammatory cell infiltration. Also, an apparent decline in the quantity of collagen, glycogen, and the number of mast cells was settled.

These findings were additionally confirmed by the concomitant morphometric measurements in the current study. A 4-week recovery led to a non-statistically significant difference (regarding collagen) or only displayed low significant differences (in the case of glycogen content, mast cell number per mm² and Vimentin immunoevaluating) when contrasting to the control group.

An important information regarding the exact BPA-persuaded cell and tissue damage mechanisms and the reversibility processes was sparked by the studies made by^[19, 20] who revealed that, the BPA hazardous impact on the epididymis and liver, respectively, were also reversed.

It has been long believed that, in adults, cardiomyocytes were terminally differentiated cells that had been permanently disengaged from the cell cycle. Though the

inability of these cells to divide, yet, they could carry out their physiological function, experience cell hypertrophy, and eventually decrease by apoptosis and/or necrosis^[68].

Given the knowledge that, both cardiomyocyte's apoptosis and necrosis are considered natural mechanisms of the organ's wear and tear that increase dramatically with age and heart pathology, the challenge question concerning the newly formed cardiomyocyte's sources necessary for structural and functional myocardial preservation has been raised. It was evidenced that, the main source of cardiomyocyte replacement following its injury is the already-existing cardiomyocytes^[69].

Numerous potential mechanisms for cardiomyogenesis in the adult heart were acknowledged. Since they are not terminally differentiated post-mitotic cells, cardiomyocytes could be able to re-enter the cell cycle and divide; Existing cardio myocytes could undergo *in-vivo* dedifferentiation and develop an embryonic replicating cell type; New cardiac myocytes could be generated from resident CSCs (cardiac stem cells) that control the physiological cellular turnover and cardiac repair following injury; Also, they could be produced when circulating hematopoietic stem cells (HSCs) engraft and transdifferentiate into cardiomyocytes^[70]. Furthermore, by altering their cell cycle, various signaling pathways, endogenous genes, and environmental factors, terminally differentiated cardiomyocytes can enter the cell cycle again and divide^[71].

CONCLUSION

In conclusion, chronic high-dosed BPA exposure could produce significant structural and functional cardiac alterations that might be due to the oxidative stress impact on the heart tissue. After ceasing exposure, BPA-induced cardiac changes became mostly reversible. Nevertheless, the particular mechanisms involving bisphenol a cardiac adverse effects and subsequent recovery are still unclear and require further research.

CONFLICT OF INTERESTS

There are no conflicts of interest.

REFERENCES

- Almeida S, Raposo A, Almeida-González M, Carrascosa C. Bisphenol A: Food Exposure and Impact on Human Health. *Compr Rev Food Sci Food Saf.* 2018 Nov;17(6):1503-1517.
- Löfroth M, Ghasemimehr M, Falk A, Vult von Steyern P. Bisphenol A in dental materials- existence, leakage and biological effects. *Heliyon.* 2019 May 27;5(5):e01711.
- Leslie, H.A.; van Velzen, M.J.M.; Brandsma, S.H.; Vethaak, A.D.; Garcia-Vallejo, J.J.; Lamoree, M.H. Discovery and quantification of plastic particle pollution in human blood. *Environ. Int.* 2022, 163, 107199. [CrossRef] [PubMed]
- Bernier MR, Vandenberg LN. Handling of thermal paper: Implications for dermal exposure to bisphenol A and its alternatives. *PLoS One* 2017 Jun 1;12(6):e0178449. doi: 10.1371/journal.pone.0178449. PMID: 28570582; PMCID: PMC5453537.
- Inoue H, Kemanai S, Sano C, Kato S, Yokota H, Iwano H. Bisphenol A glucuronide/sulfate diconjugate in perfused liver of rats. *J Vet Med Sci.* 2016;78(5):733-737. doi:10.1292/jvms.15-0573.
- Cimmino I, Fiory F, Perruolo G, Miele C, Beguinot F, Formisano P, Oriente F. Potential Mechanisms of Bisphenol A (BPA) Contributing to Human Disease. *Int J Mol Sci.* 2020 Aug 11;21(16):5761. doi: 10.3390/ijms21165761. PMID: 32796699; PMCID: PMC7460848.
- Hines, E.P.; Mendola, P.; von Ehrenstein, O.S.; Ye, X.; Calafat, A.M.; Fenton, S.E. Concentrations of environmental phenols and parabens in milk, urine and serum of lactating North Carolina women. *Reprod. Toxicol.* 2015, 54, 120–128
- Bruno KA, Mathews JE, Yang AL, *et al.* BPA Alters Estrogen Receptor Expression in the Heart After Viral Infection Activating Cardiac Mast Cells and T Cells Leading to Perimyocarditis and Fibrosis. *Front Endocrinol (Lausanne).* 2019; 10:598. Published 2019 Sep 4. doi:10.3389/fendo.2019.00598.
- Khan NG, Correia J, Adiga D, Rai PS, Dsouza HS, Chakrabarty S, Kabekkodu SP. A comprehensive review on the carcinogenic potential of bisphenol A: clues and evidence. *Environ Sci Pollut Res Int.* 2021 Apr;28(16):19643-19663. doi: 10.1007/s11356-021-13071-w. Epub 2021 Mar 5. PMID: 33666848; PMCID: PMC8099816.
- Ramadan, M.; Cooper, B.; Posnack, N.G. Bisphenols and phthalates: Plastic chemical exposures can contribute to adverse cardiovascular health outcomes. *Birth Defects Res.* 2020, 112, 1362–1385.
- Wehbe Z, Nasser SA, El-Yazbi A, Nasreddine S, Eid AH. Estrogen and Bisphenol A in Hypertension. *Curr Hypertens Rep.* 2020 Feb 29;22(3):23. doi: 10.1007/s11906-020-1022-z. PMID: 32114652.
- García-Arévalo M, Lorza-Gil E, Cardoso L, Batista TM, Araujo TR, Ramos LAF, Areas MA, Nadal A, Carneiro EM, Davel AP. Ventricular Fibrosis and Coronary Remodeling Following Short-Term Exposure of Healthy and Malnourished Mice to Bisphenol A. *Front Physiol.* 2021 Apr 12;12:638506. doi:10.3389/fphys.2021.638506. PMID: 33912069; PMCID: PMC8072349.
- Kim MJ, Moon MK, Kang GH, *et al.* Chronic exposure to bisphenol A can accelerate atherosclerosis in high fat-fed apolipoprotein E knockout mice. *Cardiovasc Toxicol.* 2014;14(2):120-128. doi:10.1007/s12012-013-9235-x,

14. Zhang YF, Shan C, Wang Y, Qian LL, Jia DD, Zhang YF, Hao XD, Xu HM. Cardiovascular toxicity and mechanism of bisphenol A and emerging risk of bisphenol S. *Sci Total Environ.* 2020 Jun 25; 723:137952. doi: 10.1016/j.scitotenv.2020.137952. Epub 2020 Mar 18. PMID: 32213405.
15. Brown AR, Green JM, Moreman J, Gunnarsson LM, Mourabit S, Ball J, Winter MJ, Trznadel M, Correia A, Hacker C, Perry A, Wood ME, Hetheridge MJ, Currie RA, Tyler CR. Cardiovascular Effects and Molecular Mechanisms of Bisphenol A and Its Metabolite MBP in Zebrafish. *Environ Sci Technol.* 2019 Jan 2;53(1):463-474. doi: 10.1021/acs.est.8b04281. Epub 2018 Dec 20. PMID: 30520632; PMCID: PMC6333396.
16. Filice M, Leo S, Mazza R, Amelio D, Garofalo F, Imbrogno S, Cerra MC, Gattuso A. The heart of the adult goldfish *Carassius auratus* as a target of bisphenol a: a multifaceted analysis. *Environ Pollut.* 2021; 269:116177.
17. Bahey NG, Abd Elaziz HO, Elsayed Gadalla KK. Potential Toxic Effect of Bisphenol A on the Cardiac Muscle of Adult Rat and the Possible Protective Effect of Omega-3: A Histological and Immunohistochemical Study. *J Microsc Ultrastruct.* 2019 Jan-Mar;7(1):1-8. doi: 10.4103/JMAU.JMAU_53_18. PMID: 31008050; PMCID: PMC6442328.
18. Eweda SM, Newairy AS, Abdou HM, Gaber AS. Bisphenol A-induced oxidative damage in the hepatic and cardiac tissues of rats: the modulatory role of sesame lignans. *Exp Therap Med.* 2020; 19:33–44.
19. Hegazy A, Omar A, Hussein Y, Abdul Rahman M, El-Bestawy E. Effect of bisphenol A on corpus epididymis and chromosomal pattern of adult rats. *ZUMJ.* 2017; 23: 1–11.
20. Amin MAS, Sonpol HMA, Gouda, RHE, Aboregela A M. Bisphenol A enhances apoptosis, fibrosis, and biochemical fluctuations in the liver of adult male rats with possible regression after recovery. *The Anatomical Record.* 2023; 306(1):213–225. <https://doi.org/10.1002/ar.25032>
21. Albus, U. (2012). *Guide for the care and use of laboratory animals* (8th ed.). SAGE Publications.
22. Institutional Animal Care and Use Committee (IACUC), Office of Research Compliance (ORC) (2013): *Nonpharmaceutical and Pharmaceutical Grade Compounds in Research Animals.* <https://research.iu.edu/doc/compliance/animal-care/bloomington/iubiacuc-nonpharmaceutical-and-pharmaceutical-grade-compounds-in-research-animals.pdf>
23. Nemzek J, Bolgos G, Williams, B *et al.* Differences in normal values for murine white blood cell counts and other hematological parameters based on sampling site. *Inflammation Research.* 2001; 50: 523–527.
24. Bancroft J D. *Theory and practice of histological techniques.* 8th Edition, Philadelphia, PA: Churchill Livingstone Elsevier Health Sciences. 2008 (8): 274–280.
25. Ramos-Vara JA, Kiupel M, Baszler T, Bliven L, Brodersen B, Chelack B, Czub S, Del Piero F, Dial S, Ehrhart EJ, Graham T, Manning L, Paulsen D, Valli VE, West K. American Association of Veterinary Laboratory Diagnosticians Subcommittee on Standardization of Immunohistochemistry. Suggested guidelines for immunohistochemical techniques in veterinary diagnostic laboratories. *J Vet Diagn Invest.* 2008 Jul;20(4):393-413. doi: 10.1177/104063870802000401. PMID: 18599844.
26. Abd El-Haleem MR, Abass MA. Effect of bisphenol A on the myocardium of adult male albino rats and the possible role of lycopene: a histological and biochemical study. *ejh.* June 2012; 35(2):326-339 | DOI: 10.1097/01.EHX.0000414921.94640.de
27. Patel BB, Kasneci A, Bolt AM, Di Lalla V, Di Iorio MR, Raad M, *et al.* Chronic exposure to bisphenol A reduces successful cardiac remodeling after an experimental myocardial infarction in male C57bl/6n mice. *Toxicol Sci.* 2015; 146:101-15.
28. Bashandy M, Zedan O. 'Role of Alpha Lipoic Acid on Cyclophosphamide Induced Cardiotoxicity in Adult Male Albino Rat: Histological Study'. *ejh.* 2019; 42(4): 888-899. doi: 10.21608/ejh.2019.12158.1114
29. Ali FAZ, Abdellah N, Hafez L., El-Ghoneimy A. Sesame Oil Ameliorates Gentamicin-induced Cardiotoxicity in Wistar Albino Rats. *Journal of Advanced Veterinary Research.* Apr. 2020;10(2): 81-87.
30. Abdelatty A, Ahmed MS, Abdel-Kareem MA, Dmerdash M, Mady R, Saad AS, Albrakati A, Elmahallawy EK, Elsayak A, Abdo W. Acute and Delayed Doxorubicin-Induced Myocardiotoxicity Associated with Elevation of Cardiac Biomarkers, Depletion of Cellular Antioxidant Enzymes, and Several Histopathological and Ultrastructural Changes. *Life (Basel).* 2021 Aug 27;11(9):880. doi: 10.3390/life11090880.
31. Kumar V, Abbas AK, Aster JC. *Robbins basic pathology.* 9th ed. Philadelphia: Saunders. 2013: 1-28.
32. Dubey A, Goswami M, Yadav K, Chaudhary D. Oxidative stress and nano-toxicity induced by TiO₂ and ZnO on WAG Cell Line. *PLoS One* 2015;10 (5): e0127493.
33. Reis-Mendes A, Padrão AI, Duarte JA, Gonçalves-Monteiro S, Duarte-Araújo M, Remião F, Carvalho F, Sousa E, Bastos ML, Costa VM. Role of Inflammation and Redox Status on Doxorubicin-Induced Cardiotoxicity in Infant and Adult CD-1 Male Mice. *Biomolecules.* 2021 Nov 19;11(11):1725. doi: 10.3390/biom11111725. PMID: 34827723; PMCID: PMC8615472.

34. Miller MA, Zachary JF. Mechanisms and Morphology of Cellular Injury, Adaptation, and Death. *Pathologic Basis of Veterinary Disease*. 2017; 2–43. e19. doi: 10.1016/B978-0-323-35775-3.00001-1. Epub 2017 Feb 17. PMID: PMC7171462.
35. Shankar A, Teppala S, Sabanayagam C. Bisphenol A and peripheral arterial disease: Results from the NHANES. *Environ Health Perspect*. 2012; 120:1297-300.
36. Gao X, Wang HS. Impact of bisphenol a on the cardiovascular system - epidemiological and experimental evidence and molecular mechanisms. *Int J Environ Res Public Health*. 2014 Aug 15;11(8):8399-413. doi: 10.3390/ijerph110808399. PMID: 25153468; PMID: PMC4143868.
37. Klint H, Lejonklou MH, Karimullina E, Rönn M, Lind L, Lind PM, *et al*. low-dose exposure to bisphenol A in combination with fructose increases expression of genes regulating angiogenesis and vascular tone in juvenile Fischer 344 rat cardiac tissue. *Ups J Med Sci*. 2017; 122:20-7.
38. Zaghoul S, Abou Elnour R, Abdelfattah M and Ismail D. Comparative histological study on the effect of mesenchymal stem cell and losartan on cardiac injury induced by doxorubicin in male albino rats. *ejh*. 2020;42(4):815-25.
39. Dabravolski SA, Khotina VA, Omelchenko AV, Kalmykov VA, Orekhov AN. The Role of the VEGF Family in Atherosclerosis Development and Its Potential as Treatment Targets. *Int J Mol Sci*. 2022 Jan 15;23(2):931. doi: 10.3390/ijms23020931. PMID: 35055117; PMID: PMC8781560.
40. Chen L, Deng H, Cui H, Fang J, Zuo Z, Deng J, Li Y, Wang X and Zhao L. Inflammatory responses and inflammation-associated diseases in organs. *Oncotarget*. 2018;9(6):7204-18.
41. García-Arévalo M, Lorza-Gil E, Cardoso L, Batista TM, Araujo TR, Ramos LAF, Areas MA, Nadal A, Carneiro EM and Davel AP. Ventricular Fibrosis and Coronary Remodeling Following Short-Term Exposure of Healthy and Malnourished Mice to Bisphenol A. *Front. Physiol*. 2021; 12:638506. doi: 10.3389/fphys.2021.638506
42. Hu Y, Zhang L, Wu X, Hou L, Li Z, Ju J, *et al*. Bisphenol A, an environmental estrogen-like toxic chemical, induces cardiac fibrosis by activating the ERK1/2 pathway. *Toxicol Lett*. 2016;250-251:1-9.
43. Smiley D, Smith MA, Carreira V, Jiang M, Koch SE, Kelley M, *et al*. Increased fibrosis and progression to heart failure in MRL mice following ischemia/reperfusion injury. *Cardiovasc Pathol*. 2014;23: 327-334.
44. Levick SP, Widiapradja A. Mast Cells: Key Contributors to Cardiac Fibrosis. *Int J Mol Sci*. 2018 Jan 12;19(1):231. doi: 10.3390/ijms19010231. PMID: 29329223; PMID: PMC5796179.
45. Rodrigues PG, Miranda-Silva D, Costa SM, Barros C, Hamdani N, Moura C, Mendes MJ, Sousa-Mendes C, Trindade F, Fontoura D, Vitorino R, Linke WA, Leite-Moreira AF, Falcão-Pires I. Early myocardial changes induced by doxorubicin in the nonfailing dilated ventricle. *Am J Physiol Heart Circ Physiol*. 2019 Mar 1;316(3):H459-H475. doi: 10.1152/ajpheart.00401.2018. Epub 2018 Dec 7. PMID: 30525890.
46. Li X, Geng J, Zhao J, Ni Q, Zhao C, Zheng Y, Chen X, Wang L. Trimethylamine N-Oxide Exacerbates Cardiac Fibrosis via Activating the NLRP3 Inflammasome. *Front Physiol*. 2019 Jul 9; 10:866. doi: 10.3389/fphys.2019.00866. PMID: 31354519; PMID: PMC6634262.
47. Carbone F, Bonaventura A, Montecucco F. Neutrophil-Related Oxidants Drive Heart and Brain Remodeling After Ischemia/Reperfusion Injury. *Front Physiol*. 2020 Feb 4;10:1587. doi: 10.3389/fphys.2019.01587. PMID: 32116732; PMID: PMC7010855.
48. Caporizzo MA, Chen CY, Prosser BL. Cardiac microtubules in health and heart disease. *Exp Biol Med (Maywood)*. 2019 Nov;244(15):1255-1272. doi: 10.1177/1535370219868960. Epub 2019 Aug 9. PMID: 31398994; PMID: PMC6880149.
49. Kuznetsov AV, Javadov S, Grimm M, Margreiter R, Ausserlechner MJ, Hagenbuchner J. Crosstalk between Mitochondria and Cytoskeleton in Cardiac Cells. *Cells*. 2020 Jan 16;9(1):222. doi: 10.3390/cells9010222. PMID: 31963121; PMID: PMC7017221.
50. Stewart TA, Yapa KT, Monteith GR. Altered calcium signaling in cancer cells. *Biochim Biophys Acta*. 2015 Oct;1848(10 Pt B):2502-11. doi: 10.1016/j.bbmem.2014.08.016. Epub 2014 Aug 20. PMID: 25150047.
51. O'Brien E, Dolinoy DC, Mancuso P. Perinatal bisphenol A exposures increase production of pro-inflammatory mediators in bone marrow-derived mast cells of adult mice. *J Immunotoxicol*. 2014; 11:205-12.
52. Ingason AB, Mechet F, Atacho DAM, Steingrímsson E, Petersen PH. Distribution of mast cells within the mouse heart and its dependency on Mitf. *Mol Immunol*. 2019 Jan; 105:9-15. doi: 10.1016/j.molimm.2018.11.009. Epub 2018 Nov 22. PMID: 30471646.
53. Mohamed D, Nor-Eldin E. Histological and immunohistochemical study of the possible protective effect of folic acid on the methotrexate- induced cardiac muscle toxicity in male albino rats. *ejh*. 2018; 41(1): 73-82. doi: 10.21608/EJH.2017.7523

54. Giordano C, Perli E, Orlandi M, Pisano A, Tuppen HA, He L, Ierinò R, Petruzzello L, Terzi A, Autore C, Petrozza V, Gallo P, Taylor RW, d'Amati G. Cardiomyopathies due to homoplasmic mitochondrial tRNA mutations: morphologic and molecular features. *Hum Pathol.* 2013 Jul;44(7):1262-70. doi: 10.1016/j.humpath.2012.10.011. Epub 2013 Jan 17. PMID: 23332932.
55. Milutinović A, Zorc-Plesković R. Glycogen accumulation in cardiomyocytes and cardiotoxic effects after 3NPA treatment. *Bosn J Basic Med Sci.* 2012 Feb;12(1):15-9. doi: 10.17305/bjbms.2012.2525. PMID: 22364298; PMCID: PMC4362411.
56. Lombo M, Herraes MP. Paternal Inheritance of Bisphenol A Cardiotoxic Effects: The Implications of Sperm Epigenome. *Int. J.Mol. Sci.* 2021;22: 2125. [CrossRef]
57. Faheem NM, El Askary A, Gharib AF. Lycopene attenuates bisphenol A-induced lung injury in adult albino rats: a histological and biochemical study. *Environ Sci Pollut Res Int.* 2021 Sep; 28(35):49139-49152. doi: 10.1007/s11356-021-14140-w. Epub 2021 May 1. PMID: 33932206.
58. Huang FM, Chang YC, Lee SS, Yang ML, Kuan YH. Expression of pro-inflammatory cytokines and mediators induced by Bisphenol A via ERK-NF κ B and JAK1/2-STAT3 pathways in macrophages. *Environ Toxicol.* 2019 Apr;34(4):486-494. doi: 10.1002/tox.22702. Epub 2019 Jan 4. PMID: 30609183.
59. Liu T, Zhang L, Joo D, Sun SC. NF- κ B signaling in inflammation. *Signal Transduct Target Ther.* 2017; 2: 17023-. doi: 10.1038/sigtrans.2017.23. Epub 2017 Jul 14. PMID: 29158945; PMCID: PMC5661633.
60. Fiordelisi A, Iaccarino G, Morisco C, Coscioni E, Sorriento D. NF κ B is a Key Player in the Crosstalk between Inflammation and Cardiovascular Diseases. *Int J Mol Sci.* 2019 Mar 30;20(7):1599. doi: 10.3390/ijms20071599. PMID: 30935055; PMCID: PMC6480579.
61. Karunarathne WAHM, Molagoda IMN, Choi YH, Park SR, Lee S, Kim GY. Bisphenol A: A potential Toll-like receptor 4/myeloid differentiation factor 2 complex agonist. *Environ Pollut.* 2021 Jun 1; 278:116829. doi: 10.1016/j.envpol.2021.116829. Epub 2021 Mar 1. PMID: 33706241.
62. Valokola MG, Karimi G, Razavi BM, Kianfar M, Jafarian AH, Jaafari MR, Imenshahidi M. The protective activity of nanomicelle curcumin in bisphenol A-induced cardiotoxicity following subacute exposure in rats. *Environ Toxicol.* 2019; 34:319–329.
63. Amjad S, Rahman MS, Pang MG. Role of Antioxidants in Alleviating Bisphenol A Toxicity. *Biomolecules.* 2020 Jul 25;10(8):1105. doi: 10.3390/biom10081105. PMID: 32722388; PMCID: PMC7465987.
64. Mączka W, Grabarczyk M, Wińska K. Can Antioxidants Reduce the Toxicity of Bisphenol? *Antioxidants (Basel).* 2022 Feb 18;11(2):413. doi: 10.3390/antiox11020413. PMID: 35204295; PMCID: PMC8869647.
65. Meli R, Monnolo A, Annunziata C, Pirozzi C, Ferrante MC. Oxidative Stress and BPA Toxicity: An Antioxidant Approach for Male and Female Reproductive Dysfunction. *Antioxidants (Basel).* 2020 May 10;9(5):405. doi: 10.3390/antiox9050405. PMID: 32397641; PMCID: PMC7278868.
66. Fonseca MI, Lorigo M, Cairrao E. Endocrine-Disrupting Effects of Bisphenol A on the Cardiovascular System: A Review. *J Xenobiot.* 2022 Jul 13;12(3):181-213. doi: 10.3390/jox12030015. PMID: 35893265; PMCID: PMC9326625.
67. Berger A, Ziv-Gal A, Cudiamat J, Wang W, Zhou C, Flaws JA. The effects of in utero bisphenol A exposure on the ovaries in multiple generations of mice. *Reprod Toxicol.* 2016 Apr; 60:39-52. doi: 10.1016/j.reprotox.2015.12.004. Epub 2015 Dec 30. PMID: 26746108; PMCID: PMC4866900.
68. Laflamme MA, Murry CE. Heart regeneration. *Nature.* 2011; 473:326– 335. doi:10.1038/nature10147.
69. Senyo SE, Steinhauser ML, Pizzimenti CL, Yang VK, Cai L, Wang M, Wu T, Lechene CP, Lee RT, Guerquin-Kern J-L, Lechene CP, Lee RT. Mammalian heart renewal by pre-existing cardiomyocytes. *Nature.* 2012;493(7432):433–436.
70. Leri A, Rota M, Pasqualini FS, Goichberg P, Anversa P. Origin of cardiomyocytes in the adult heart. *Circ Res.* 2015 Jan 2;116(1):150-66. doi: 10.1161/CIRCRESAHA.116.303595. Erratum in: *Circ Res.* 2015 Dec 4;117(12): e133. PMID: 25552694; PMCID: PMC4283577.
71. Johnson J, Mohsin S, Houser SR. Cardiomyocyte Proliferation as a Source of New Myocyte Development in the Adult Heart. *Int J Mol Sci.* 2021 Jul 21;22(15):7764. doi: 10.3390/ijms22157764. PMID: 34360531; PMCID: PMC8345975.

الملخص العربي

التعرض لمادة البيسفينول أ يؤدي إلى زيادة موت الخلايا المبرمج والالتهاب والتليف في قلب الجرذ البالغ مع إمكانية التحسن بعد التعافي

أمل سليمان سويلم وإيمان محمد أحمد عبد الغنى و محمد أحمد صبرى

قسم التشريح الأدمي والأجنة - كلية الطب البشرى - جامعة الزقازيق - مصر

لخلفية: يعتبر البيسفينول أ (BPA) ملوثاً بيئياً ذا استخدام عالمي كمادة ملدنة. يبدأ التعرض اليومي للبيسفينول أ مبكراً قبل الولادة ويستمر طوال حياة الشخص دون حد أو إنذار للسلامة المتعلقة بالصحة العامة.

الهدف: استكشاف السمية القلبية المحتملة للبيسفينول أ (BPA) الذي يتم تناوله عن طريق الفم في الفئران البالغة ، ولتقييم نتائج فترة التعافي بعد توقف البيسفينول أ .

المواد والطرق المستخدمة: فى هذا البحث تم تقسيم ثمانية و أربعين من ذكور الجرذان البيضاء البالغة إلى أربع مجموعات (اثنى عشر لكل مجموعة) و هى على التوالي المسيطرة السلبية ، المسيطرة الإيجابية ، المعالجة بـ البيسفينول أ و المجموعة المتعافية. تلقت الفئران فى المجموعة الثالثة البيسفينول أ لمدة ثمانية أسابيع يومياً (٥٠ مجم / كجم من وزن الجسم ، عن طريق الأنبوب المعدى بالحقن عن طريق الفم). ، أما فى مجموعة التعافى فقد تلقت الحيوانات البيسفينول أ ، على غرار المجموعة الثالثة ، ثم تُركت لتتعافى دون إعطاء البيسفينول أ لمدة ٤ أسابيع. فى نهاية التجربة ، تم جمع الدم لتقدير مستوى مصل الكرياتينين كيناز - (CK-MB) كما تم التعامل مع عينات القلب من أجل دراسة الأنسجة ، والكيمياء النسيجية المناعية ، والقياس الشكلى الكمي.

النتائج: أحدث البيسفينول أ العديد من التغييرات النسيجية والكيميائية المناعية والكيميائية الحيوية التي تجلت فى اضطراب ألياف القلب ، واحتقان الأوعية الدموية ، والنزيف ، وتسرب كرات الدم الحمراء ، وتسلل الخلايا الالتهابية والتليف . كما ظهر الساركوبلازم الخاص بعضلات القلب باللون الحمضي الداكن ، أما النواة فقد اظهرت تصلبا و فراغا من حولها. بالإضافة لما سبق فقد كانت النسبة المئوية لمتوسط المساحة لترسب ألياف الكولاجين ومحتوى الجليكوجين وبروتين X المرتبط بـ ٢-Bcl (BAX) والعامل النووي كابا ب(NFkB) والتعبيرات المناعية للفيمنتين (Vimentin) مرتفعة بشكل ملحوظ. أيضا تم زيادة عدد الخلايا البدينة / مم مربع كما ارتفعت مستويات MDA و CK-MB وفي الوقت نفسه انخفضت مستويات SOD و GSH و CAT. أما بعد التعافى لمدة أربعة أسابيع ، فقد أظهرت التغييرات الخاصة بعضلات القلب والأوعية الدموية تحسناً ملحوظاً وكما تم توجيه جميع المقاييس السابقة نحو القيم الطبيعية ، إلا أن أن معظمها ما زال يُظهر اختلافات كثيرة منخفضة مقارنةً بالمجموعات الضابطة.

الخلاصة: تسبب البيسفينول أ فى السمية القلبية الهيكلية والوظيفية للقلب عن طريق توليد أنواع الاكسجين التفاعلية والالتهاب والاستماتة . و قد أظهرت عضلة القلب تحسناً ذاتياً كبيراً بعد انسحاب البيسفينول أ مما يدل على أن الآثار الجانبية له ذات ضرر عابر. و بالرغم من ذلك ، فإن الآليات الخاصة الكامنة وراء السمية القلبية أو الشفاء لا تزال تتطلب مزيداً من الدراسة.